CHEMICAL ENGINEERING TRANSACTIONS
VOL. 33, 2013
A publication of AIDIC
The Italian Association of Chemical Engineering
Online at: www.aidic.it/cet
Guest Editors: Enrico Zio, Piero Baraldi

ISBN 978-88-95608-24-2; **ISSN** 1974-9791
DOI: 10.3303/CET1333166

Prognostic Health Management (PHM) of Electrical Systems using Conditioned-based Data for Anomaly and Prognostic Reasoning

James P. Hofmeister, Robert S. Wagoner, Douglas L. Goodman*

Ridgetop Group, Inc., 3580 West Ina Road, Tucson,Arizona, 85741, USA
doug.goodman@ridgetopgroup.com

Electrical systems, such as those consisting of electrical power driving motors and actuators, are varied and include industrial, aerospace, and automotive applications. These power systems are critical and must provide stable operating voltages for various modules found throughout the host system, including electromechanical actuators (Goodman et al., 2007), CPU-based control systems, and widely varying loads. Operating temperatures can vary as well, with vibration and mechanical shock conditions adding further stress and degradation of components in the power system. A key advantage of electronic prognostics is the monitoring of health of a power system in these critical systems. With prognostics, impending failure can be detected and mitigated. In addition, the prognostics and health management (PHM) system can help optimize the support logistics and reduce costs.
In this paper, an overview of signature-based PHM technology to detect anomalies and prognostic reasoning is presented: A signature is extracted from condition-based data and is called a fault-to-failure progression (FFP) signature. Thereafter, a representative PHM system that extracts and processes dynamic degradation signatures for a critical DC regulated power system is described. The hardware and software integration involved with the addition of advanced PHM functionality to a host system is discussed, along with resulting output display and data that can be used to provide dynamic state-of-health (SoH) and remaining useful life (RUL) estimates.

1. Introduction

Prognostic health management (PHM) systems can support the timely mitigation of faults found in complex systems before catastrophic failures occur. Complex systems often incorporate data buses, which can be non-invasively monitored to extract condition-based fault-to-failure progression (FFP) signatures which can be processed to detect degradation, and used to provide estimates of remaining useful life (RUL) and state-of-health (SoH) of the system (Goodman, 2007, pp. 1902-1906). To illustrate this capability, this paper presents results from a Model-based Analysis and Prognostic Reasoner (MAPR) that Ridgetop Group, Inc. is developing for a NASA-sponsored (U.S. National Aeronautics and Space Administration) Small Business Innovation Research (SBIR) program (contract NNX11CA04C, 12 June 2011 to 11 June 2013).

1.1 Benefits of PHM-enabled systems

The motivations for PHM-enabling systems include the following: (1) prognostics provides advanced warning of impending failure conditions on critical systems and avoidance of expensive system down-time; (2) Physical evidence of degradation is the basis for maintenance on the system, not an arbitrary time interval; (3) PHM can reduce support costs through optimized timing of service and parts replacement; and (4) Autonomic Logistics Information Systems (ALIS) can be established, placing spare parts and provisions where needed.
Diagnostics indicates the state of the system to perform its designed function, while prognostics predict when a system is likely to fail. Predictive diagnostics incorporates sensors (existing or additive), data collection routines, and algorithms that provide state-of-health (SoH) and remaining useful life (RUL) of the

Please cite this article as: Hofmeister J., Wagoner R., Goodman D., 2013, Prognostic health management (phm) of electrical systems using condition-based data for anomaly and prognostic reasoning, Chemical Engineering Transactions, 33, 991-996
DOI: 10.3303/CET1333166

system under observation. Wear-out conditions can vary widely, depending on the environment in which the systems are placed so evidence-based indications are valuable. Health Management, in turn, takes the prognostics and utilizes the predictive capabilities to schedule maintenance when the system is taken off line. This reduces the overall life cycle cost of the system.

1.2 Complex systems

Systems can assume a multi-level hierarchy spanning at least five levels: (1) IC (or die); (2) components; (3) boards; (4) module/assembly; (5) system and system-of-systems: a fault can occur in any level and propagate into a system failure. From a practical perspective, state information is extracted as non-intrusively as possible utilizing existing sensors and data measurements.

1.3 Illustrative example of a complex system

Figure 1 is an illustrative example of a complex system which is PHM-enabled and which consists of the following: (1) a 24 VDC switch-mode power supply (SMPS); (2) a brushless DC motor (BLDC); and (3) PHM executable software. There is a single DC voltage output sensor and three AC current sensors – all non-invasive (see Figure 2). Data are acquired and placed onto a data bus, and algorithms are used to condition and process the data to extract multiple FFP signatures (one for each fault mode): the power supply has one fault mode (loss of filtering capacitance); the servo control for the motor has six fault modes (the six power switching transistors used to produce the motor currents); and the motor load has one fault mode (excessive load current). The FFP signatures are then processed by Kalman Filter algorithms to remove noise. For each set of captured data (time-stamped data), the multiple FFP signatures are then processed by an advanced time-to-failure (ATTF™) kernel program which adapts FFP signature models to the input data. Each adapted FFP signature model is used to produce RUL estimates and, in turn, the RUL estimates are used to produce SoH estimates. The RUL and SoH results are further processed to identify which fault mode is likely to cause the system to fail first: smallest RUL and smallest SoH, each having an associated fault mode. An application front-end program provides graphical user interface (GUI) support for PHM control and visualization of results. The phase currents are sampled during the positioning of the motor. The algorithms do not assume that any detected fault is independent of or dependent on any other detected fault.

2. Condition-based FFP signatures for anomaly and prognostic reasoning

When components degrade from a state of no damage to a failed state, the electronic device or assembly that is failing typically produces one or more condition-based FFP signatures.

2.1 Example FFP signature

One example, seen in Figure 2, is the well-known voltage ripple signature increase as a power supply filter fails. The data shown came from a power supply testbed that was fault-injected by automatically stepping changes in the filter capacitance: the original, noisy and stepped data (black) was signal-conditioned (blue) before processing: (1) ripple voltage measurements below a “floor” value (green) are defined as “no detectable degradation;” (2) measurements between the defined floor value and a “ceiling” value (red) are defined as “degraded;” and (3) measurements at or above the defined ceiling value are defined as “failed” and the power supply has reached the effective end of its useful life. Other signatures have been identified and characterized, including power supply feedback failure; motor/actuator failure evidenced by increase friction on the stator; metal-oxide field-effect transistor (MOSFET) failure in a motor winding circuit; and transmission line failure because of kinking and/or crushing. The challenge is to use and/or develop a non-invasive means to capture data from which at least one FFP signature can be extracted for PHM.

FFP signature data is normalized and made dimensionless to facilitate defining and using FFP signature models to support many applications. Eq(1) is used to convert FFP signature data into ratios of normalized values, such as those seen in Figure 2.

$$V_{R\_FFP} = (V_R - V_{RNOM})/V_{RNOM} \quad (1)$$

Where V_{R_FPP} is the normalized, dimensionless FFP signature, V_R is the measured ripple voltage, and V_{RNOM} is the nominal, non-degraded value of the ripple voltage.

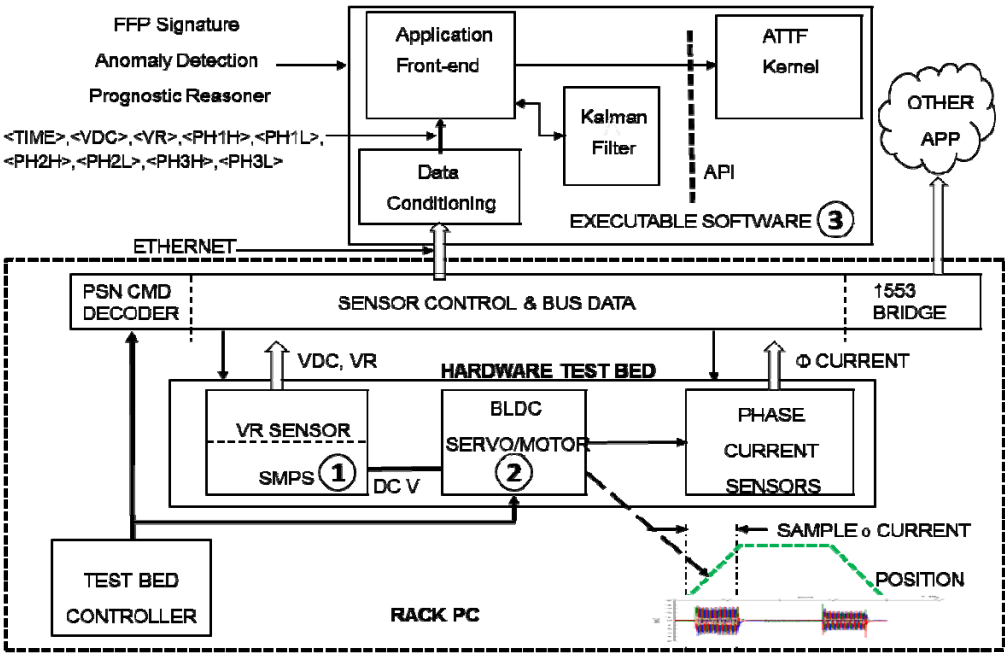

Figure 1: Architectural block diagram - testbed with executable PHM software

2.2 FFP Signature modeling

Referring to Figure 2, the creation of an FFP signature model is straightforward: (1) create a representative curve using a set of normalized, dimensionless FFP signature data; (2) divide the time between the start of detectable degradation and failure into three periods having an approximate ratio of 8:7:5; (3) measure the amplitudes at those times; and (4) specify the resulting four model points (the red circles on the plots in Figure 2) using an application programming interface (API) header file. In modeling, exact times and amplitudes are not required because an ATTF program kernel adapts the FFP model as data are received and processed.

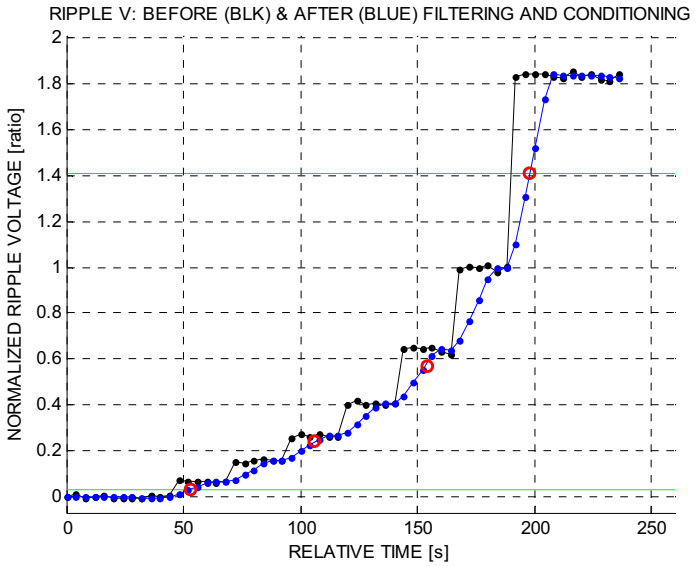

Figure 2: Example FFP signature – ripple voltage increases as power supply filter fails

2.3 Noise and Kalman Filtering

Sampled data is very noisy, especially if the ripple voltage of an SMPS is sampled, for example, thousands of times in one millisecond once every 30 minutes over a time span in the tens of thousands of minutes. After conditioning bus data into a single data point per sample, Kalman Filtering is used to remove noise to produce "clean" FFP signatures, such as the blue-dotted plot in Figure 2 of the FFP signature data after conditioning, filtering, and normalizing.

2.4 Multiple sensors and fault modes

Referring to Figure 3, multiple non-invasive, existing sensors are used to measure the three phase currents from which seven FFP signatures are extracted for the following fault modes: increase in on-resistance of any one of the six power-switching MOSFETs (six FFP signatures), and an increase in friction or weight loading on motor (one FFP signature). An 8th FFP signature for the loss of filtering capacitance is extracted from a non-invasive monitoring of the DC voltage of the power supply.

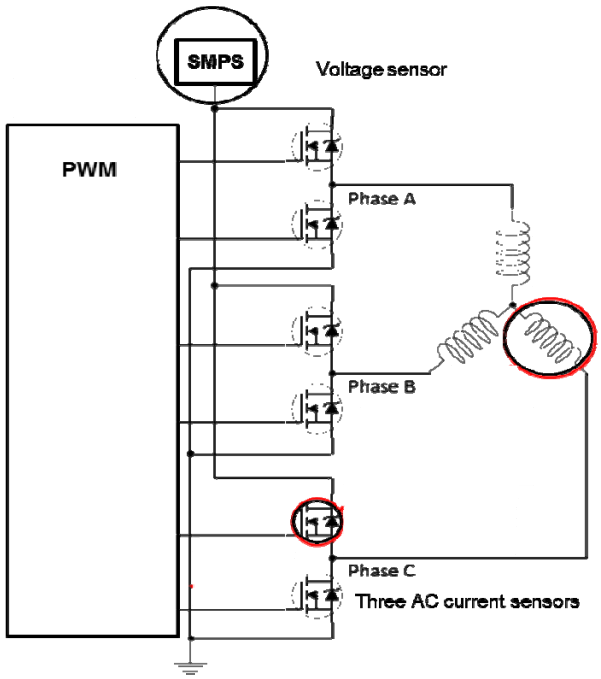

Figure 3: Simplified diagram of a power supply and brushless DC motor

3. Advanced-Time-to-Failure (ATTF) program kernel

In Figure 2, it is seen that the defined FFP signature model (the four circles) does not match the data. For each data point, except the first, received by the ATTF kernel program, the FFP signature model is adapted to the data. The adapted FFP model is then used to project a probable time-to-failure (TTF) – very much like Extended Kalman Filtering. The estimated *TTF* and the data point time (*DPT*) are then used to calculate an estimated RUL using Eq(2) and an estimated SoH value using Eq(3).

$$RUL = (TTF - DPT) \quad (2)$$

$$SoH = [1 - (FFP_{AMPL}) / (FFP_{AMPL\_FAIL} - FFP_{AMPL\_GOOD})] * 100 \quad (3)$$

Where FFP_{AMPL} is the amplitude of the data (the blue-dotted plot in Figure 2), FFP_{AMPL_FAIL} and FFP_{AMPL_GOOD} are defined by the FFP signature model.

3.1 FFP signature processing: RUL and SoH estimates, analysis of results

Figure 4 is a plot of the SoH estimates produced by ATTF for the FFP signature data shown in Figure 2; and Figure 5 is a plot of the relative accuracy of the SoH and RUL estimates. It is seen that in less than 10 data points, the ATTF algorithms converged to solution accuracy of better than 90% and better than 95% in less than 15 data points. Measurements of accuracy of RUL and SoH estimates are based on a method

of accuracy used for straight-line transfer curves, differential non-linearity (DNL), that is then used in a NASA-defined measurement of accuracy, Relative Accuracy (RA) (Saxena, 2010, 20 pages):

$$DNL_E(t) = (RUL_{IDEAL}(t) - RUL_{ESTIMATE}(t))/RUL_{IDEAL}(t) \quad (4)$$

$$RA(t) = 1 - DNL_E(t) \quad (5)$$

Where RUL_{IDEAL} (or SoH_{IDEAL}) is a point in time on the ideal RUL (or SoH) transfer curve (blue lines in Figure 4) and $RUL_{ESTIMATE}$ (or $SoH_{ESTIMATE}$) is the estimate at that point in time.

Given the noisy, stepped nature of the FFP signature data and the small size of the data set, the accuracy results for both the RUL and the SoH estimates are evaluated as excellent.

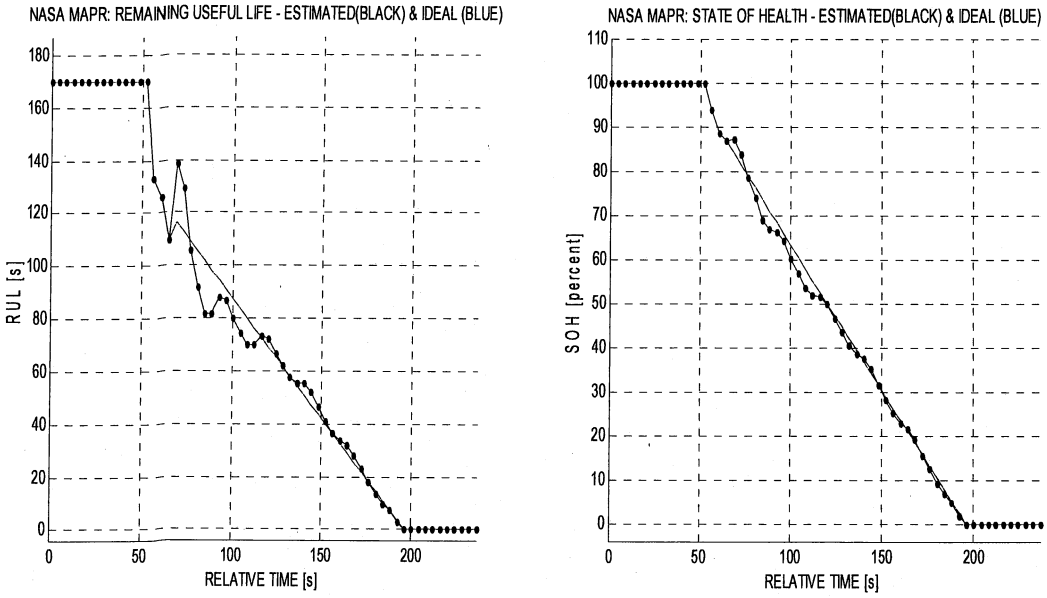

Figure 4: RUL (left-side) and SoH (right-side) estimates for the FFP signature shown in Figure 2

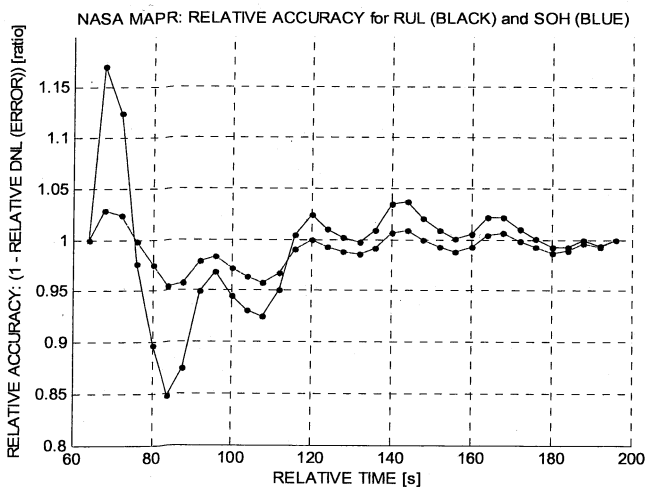

Figure 5: Relative accuracy as a ratio for the SoH and RUL estimates shown in Figure 4

3.2 System RUL and SoH

The RUL and SoH results for each FFP signature are analyzed by MAPR algorithms to calculate estimated RUL and SoH values for the system for each data point: the smallest RUL and SoH values for all of the FFP signatures. The MAPR algorithms also identify the failure mode(s): power supply filter, one or more of the six power switching MOSFETs, and/or excessive friction (load) place on the motor stator.

3.3 Training and memory

The prognostic methods presented in this paper do not require any training: FFP signature models represent prior knowledge. The methods are also not memory- or compute-intensive: all memory requirements for prognostic purposes are in less than 50 variables and constants maintained in header and trailer areas of the FFP signature model. The time to process a data set of 1344 data points was less than 180 milliseconds.

4. Basic description of the ATTF algorithms

The four model points of amplitude and time are used to calculate initial values of the amplitude coefficient A_0 and the life parameter τ in Eq(6), which is used as an FFP signature model.

$$a = A_0[1 - e^{(-t/\tau)}] \tag{6}$$

Where the data amplitude is *a* at time *t*, A_0 is the amplitude coefficient, and *t* is the life parameter.

After initialization of the model, the amplitude and time of each data point is compared to the model amplitude at time *t*. The value of the model life parameter is adjusted, and the adjusted FFP signature model is extended to produce an estimate of the time-to-failure (TTF). The estimated RUL is the difference between TTF and the current data time. An estimated SoH is determined using Eq(7).

$$SoH = 100(RUL_{EST}/TTF) \tag{7}$$

Where at time *t*, RUL_{EST} is the estimated RUL value and *TTF* is the estimated time-to-failure.

5. Conclusions

In this paper we presented benefits of PHM-enabled systems and we introduced the concept of complex systems, and discussed a specific complex system that has a switch-mode power supply, a brushless motor, and motor controls such as a Pulse Width Modulator. That system was prognostic-enabled to use condition-based data for anomaly detection and prognostic reasoning. The prognostic-enablement was achieved by accepting and processing condition-based data from the system 1553 bus; performing special data conditioning to extract FFP signatures; using Kalman Filtering to filter out noise; and then using ATTF algorithms to adapt FFP signature models to condition-based data values. For each data point, an adapted FFP signature model is used to project an estimated failure time, from which estimated RUL and SoH values are calculated. MAPR algorithms are used to evaluate the RUL and SoH results to estimate the RUL and SoH values for the system, and to identify the failure modes. The MAPR, conditioning, filtering, and ATTF algorithms do not require training; they produce fast and accurate RUL and SoH estimates.

References

Goodman, D., Hofmeister, J., Judkins, J., 2007, Electronic prognostics for switched mode power supplies, Microelectronics Reliability, 47-12, 1902-1906.

Saxena, A., Celaya, J., Saha, B., Saha, S., Goebel, K., 2010, Metrics for offline evaluation of prognostic performance, International Journal of Prognostics and Health Management, ISSN 2152-2648, 1-1, 20 pages.